

Part **IV**

**Seismogenic Zone Chaterization**

Uncorrected Proof



# Convergent Margin Structure in High-Quality Geophysical Images and Current Kinematic and Dynamic Models

Roland von Huene, C. R. Ranero and D.W. Scholl

AUI

**Abstract** Understanding the mechanics of convergent margins is fundamental to assessing risks from earthquakes and trans-oceanic tsunamis. Marine observations of the past decade have advanced that understanding. A once commonly inferred accreted wedge extending from trench axes to shelves is now resolved into 3 domains of different mechanics in space, that vary during an earthquake cycle. The frontal prism increases weight on subducting materials elevating pore fluid pressure and reducing interplate friction. The middle prism is moderately stable and merges into the more stable margin framework of the inner prism beneath the upper slope and shelf. Significant accretion occurs as material from the frontal prism is added to the middle prism. Accretion is common along thickly (>1 km) sedimented trenches and slowly converging margins. Rapid convergence enhances the efficiency of sediment subduction and subduction erosion. The subduction channel on the lower plate accepts a finite amount of trench sediment and any excess is added to the frontal prism on the upper plate. Erosion beneath the middle slope contributes material to the subduction channel. Erosion and accretion can be coeval, for instance, subducted seamounts erode the upper plate as adjacent sediment accretes. The change in strain during interseismic locking that is released during coseismic slip, changes the dynamics of each segment in time. This helps explain extensional normal faults in a converging plate environment. Recent observations provide information for a unifying framework concept to aid interpretations of both accreting and eroding margins.

**Keywords** Convergent margins • Subduction erosion • Accretion

## 1 Introduction

Many concepts regarding subduction zones were derived from interpretations of seismic data with 1970–1980s spatial resolution and depth of imaging. Examining such interpretations with scientific drilling found that 70% of the tested geophysical interpretations were fundamentally wrong. These interpretations

lacked adequate constraints and various model dependant interpretations were permissible. The high vertical exaggeration and travel-time rather than depth images in older seismic data distort structure and limit imaging of dipping reflectors. A lack of coherent structural images was commonly attributed to an inability of seismic techniques to image mélanges. Even with simple modern 3D images only 20% of a large test group of geoscientists arrived at correct tectonic interpretations in a community benchmarking exercise (Bond et al., 2007). Improved seismic imaging integrated with multibeam bathymetry reveals much more

R. von Huene  
US Geological Survey and University of California, Davis,  
4300 Carlson Way, Diamond Springs, CA 95619

structure allowing many earlier simplifying assumptions to be replaced with data and interpretations to be reconsidered. Yet tectonic models abound and no single one contains a unifying concept or model.

The original “plate tectonic” assumption that entire convergent margins form by steady state accretion producing a broad imbricate stack is replaced by observations showing segmentation of structure requiring areas with different materials and processes. Discrete margin segmentation was proposed 20 years ago (Cloos and Shreve, 1988; Taira, 1994). Recent data resolve an unstable frontal prism and a more stable middle slope, as for instance in the classical Sumatran accretionary wedge (Kopp and Kukowski, 2003) where earlier interpretations became a type example of a steadily accreting body (Hamilton, 1988). Segmentation is observed in improved seismic images at margins along the Americas and Japan (i.e., Ranero and von Huene, 2000; Christenson et al., 2003; von Huene and Ranero, 2003; Bangs et al., 2006; Ranero et al., 2006; Moore, 2007; Kimura et al., 2007). A two segment upper plate and subduction channel model introduced by Shreve and Cloos (1986) and Cloos and Shreve (1988) was based on fluid mechanics as proposed by Sorokhtin and Lobkovskiy (1976). In the subduction channel model a compressionally strained prism adjacent to the deformation front builds at the inlet where trench sediment subducts forming a subduction channel beneath the prism. Active contraction occurs mostly in this zone of compression rather than progressively across the entire margin. In the Cloos and Shreve model, the inlet controlled subduction channel thickness, and when inlet capacity was exceeded, the excess would accrete. The structural features of the model were not imaged in the seismic data of the 1970–1980 period but are now clearly observed.

The segments observed in seismic images are consistent with the Dynamic Coulomb wedge model (Wang and Hu, 2006). Conventional models are commonly without a reference to the geologic time associated with a margin’s structural development. The dynamic wedge model shows the significance of a seismic cycle in understanding subduction zone mechanics. It explains how stress can affect segments differently during a cycle. During interseismic periods when the plate interface fault locks, the margin wedge landward of the frontal prism stores the elastic strain from plate convergence. The weak material and relatively

small mass of the frontal prism cannot store much elastic strain so it is characterized by permanent deformation. During an earthquake the elastic strain released in the middle prism shoves against the frontal prism creating a coseismic pulse of deformation and elevated pore fluid pressure. This can explain features observed in multibeam seafloor morphology and depth processed seismic images. These two behaviors affect both accreting and eroding margins in similar manners.

In the literature, convergent margins are commonly divided into two pure end-members with accreting or eroding modes of mass transfer. Recent observations indicate a mix of accretion and erosion in space and time. An example is the Nankai margin where subducting seamounts erode the upper plate in an otherwise accretionary environment (Bangs et al., 2006). Despite a clear difference in mass transport, certain mechanical processes may share similarities.

## 1.1 Aims of this Chapter

In this review we expose to a broader readership the ideas advanced within a community of specialists. We develop a unifying fundamental framework in which to consider diverse observations. The major concepts we consider are the availability of trench sediment at the deformation front, the capacity of the subduction channel inlets to accept materials, the change in relative strength of the upper and lower plates, and an essential change of dynamics during coseismic and interseismic periods. We summarize kinematics in erosional and accretionary segments of the Chilean margin and relate these to convergent margin framework processes. Dynamics can be explained in accord with the dynamic Coulomb wedge concept (Wang and Hu, 2006). Differences in subduction zone behavior during interseismic locking and coseismic slip provide an explanation for puzzling observations of extensional faulting in a compressional convergent plate environment and helps to understand the paradox of a prism with contractile accretionary structure fronting eroding margins. Convergent margin structural complexity precludes a simple model that explains them all but some core concepts provide a framework that can be augmented and modified to fit the diversity of observations along various margins.

## 2 Upper Plate Rock Units

We apply non-generic terms to four upper plate rock units inferred from geology and structure in seismic images following Scholl and von Huene (2008). The generic terms “*accrete*” and “*erode*” imply material transfer between converging plates. We use them only if upper plate material provenance is known, whether sourced from the lower plate or repositioned upper plate material. Viewed from the trench axis landward (Fig. 1) the units are, (1) an actively deforming sediment body at the foot of the margin slope, the *frontal prism* which transitions into a (2) body of older and more consolidated material, the *middle prism*, and (3) the *inner prism* consisting of the margin’s rock framework. These units are covered by, (4) an overlying sedimentary *slope apron*. On the subducting lower plate, the top layer of clastic material on basement comprises the *subduction channel*. Kimura et al. (2007) recognized a similar segmentation but termed it the outer wedge, transition zone, and inner wedge.

The term frontal prism came into wider use after drilling of the Costa Rica “accretionary prism” sampled only slope sediment and no lower plate sediment (Kimura et al., 1997). Lower plate sediment was not transferred to the upper plate and the pre-drilling interpretations that all landward dipping reflections represent accreted trench sediment was incorrect. In samples, accreted sediment lithology can be non-unique because trench axis sediment is compositionally the same as its slope sediment parent. Slope sediment trapped and kneaded into the imbricating frontal prism is repositioned and not accreted. Slope sediment crossing the frontal prism to reside briefly in the trench axis can be returned to the prism as the decollement propagates seaward of the deformation front. This accreted sediment has essentially the same lithology as slope sediment making a distinction from samples alone problematical. Where material transfer between plates is uncertain the non-generic terms “frontal and middle prisms” are convenient.

### 2.1 Frontal Prism

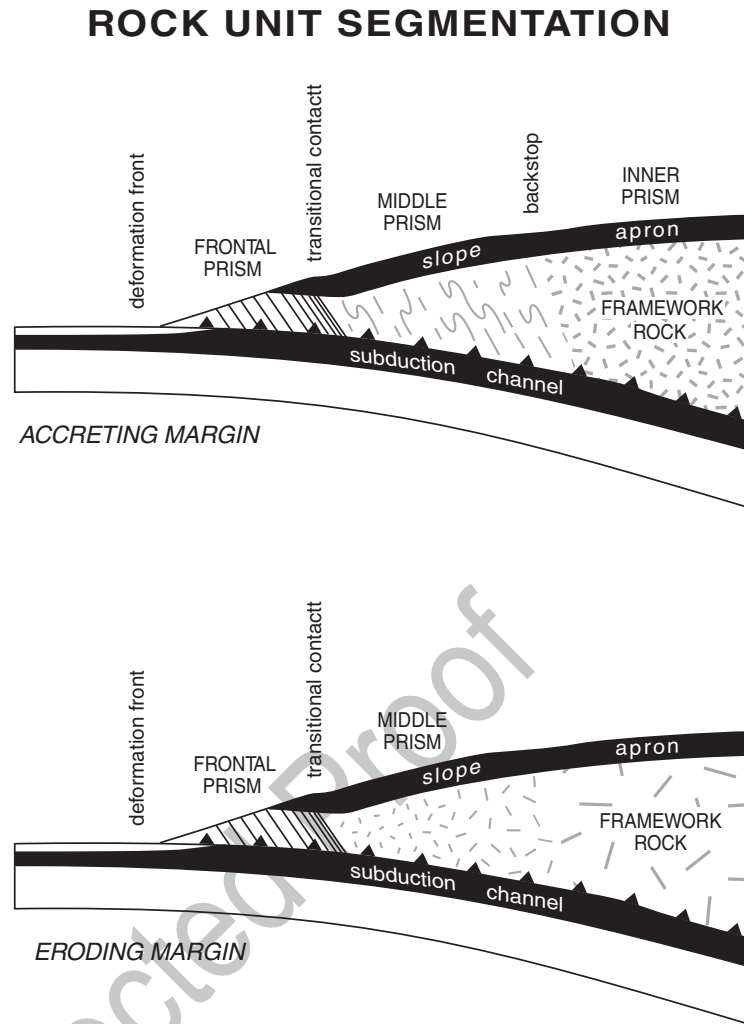
Convergent margin upper plates are bordered at the trench axis by a *frontal prism*, 5 to ~30 km wide

(Fig. 1). In many seismic images, frontal prisms contain clear landward dipping reflections that indicate tectonic thickening by imbrication. Where the complexity of internal structure exceeds resolution of the applied seismic technique an imbricate structure is commonly assumed. Scientific drilling of accretionary frontal prisms along the Barbados and Nankai drill transects has sampled oceanic sediment transferred from the subducting plate, a transfer also seen in seismic images. Off Central America, Peru, and northern Chile, the term accretionary frontal prism is inappropriate because evidence that the sampled prism sediment was transferred from the lower to the upper plate is inconclusive. The frontal prism of accretionary margins either merges up slope into a older more consolidated *middle prism* through a 1–5 km wide contact zone or is separated from the middle prism by a fault zone. This boundary has been called a backstop but it differs from the one introduced by Byrne et al. (1988) which is stationary and separates igneous from sedimentary rocks.

### 2.2 Middle Prism

In accretionary margins middle prisms may be 40–100 km wide bodies presumed to contain trench sediment transferred from the frontal prism. Their internal structure is seldom imaged well by reflection seismic surveys. The overlying slope apron displays little active permanent contractile deformation in addition to what this unit inherited during residence in the frontal prism. These prisms are commonly bounded landward by a backstop of framework rock. At erosional margins the middle prism consists of decomposed and fractured framework rock with reduced seismic velocity (e.g., Chile, Central America). The fractured framework rock structure in seismic records is difficult to distinguish from accreted sediment as shown when they were drilled (i.e., Central America and Peru). Beneath middle slopes, material has greater rigidity and greater seismic velocity than frontal prisms. Large middle prisms commonly occur where margins have had thickly (>1 km) sedimented trenches for several Myr periods and where orthogonal convergence is less than ~40–50 km/Myr (e.g., Makran, and Nankai Trough) (Clift and Vannucchi, 2004).

**Fig. 1** Rock and sediment units of convergent margins. At accreting margins the rock framework (structurally the inner prism) backs a *middle prism* of accreted material. At eroding margins coherent framework rock becomes increasingly fractured down slope to form the *middle prism*. Frontal prisms can contain upper and/or lower plate materials



### 2.3 Inner Prism: Rock Framework

The margin's core, its *rock framework*, consists of igneous or metamorphic basement and lithified sedimentary rock. These rocks are seen in coastal exposures and they extend seaward beneath the submerged margin as established with drill and surface samples. The framework rock is as diverse as Paleozoic and older igneous and metamorphic cratonic rock (i.e., Peru and Chile) and the magmatic massifs of Cenozoic arcs (i.e., Aleutian, Izu-Bonin, and Tonga). The rock framework locally contains metamorphosed fossil accretionary middle prisms. Structurally, the inner prism is strong and only broadly deformed, commonly at the edge of the shelf.

### 2.4 Slope Sediment Apron

The upper plate is covered by an apron of sediment that extends from the shelf to the lower trench slope. Scientific drilling at the erosional margins of north-east Japan, Tonga, Peru, Costa Rica, and Guatemala, revealed several km of long-term subsidence evidenced by shallow water indicators in the basal beds of the slope apron not far from the trench axis. The underlying basement surface is commonly an eroded wave-based unconformity and the overlying strata record a vertical displacement history. The thickness of aprons ranges from a few meters to 5 km (Clift and Vannucchi, 2004).

### 3. Geophysical Observations of Upper Plate Segmentation

A long standing assumption that margin wide wedges accreted linearly, consolidate, and increase in thickness up slope, fails to explain a variety of tectonic structures. In the past decade, upper plate deformational segments were resolved in multibeam seafloor morphology and in well processed seismic images (Fig. 2). In multibeam bathymetric surveys, an upper slope morphology sufficiently stable to develop many canyons changes to a moderately stable middle slope morphology and finally to the unstable frontal prism (Fig. 2a). Some associated seismic images illustrate a corresponding deterioration in reflector coherence down slope (Fig. 2c). In eroding margins, lowered seismic velocity and middle slope failure is explained as fracturing and progressive break-up of the framework rock. The presumed fractured material in an eroding margin has a seismic velocity distribution similar to the landward increased velocity resulting from sediment consolidation in an accreting one (Sallares and Ranero, 2005). Importantly, the seismic reflections in middle slope sediment aprons show little pervasive or strong permanent compressional deformation. In some drill cores the ages of little deformed strata are middle Miocene invalidating the argument that slope sedimentation is so rapid that it masks deformation (i.e., Ranero et al., 2007) Interplate shear as hundreds of km of lower plate subduct for <5 Ma should permanently deform the slope apron if the underlying middle prism were deforming significantly. The common loss of coherent slope apron reflections at the middle to frontal prism contact indicates deformation there (Fig. 2c).

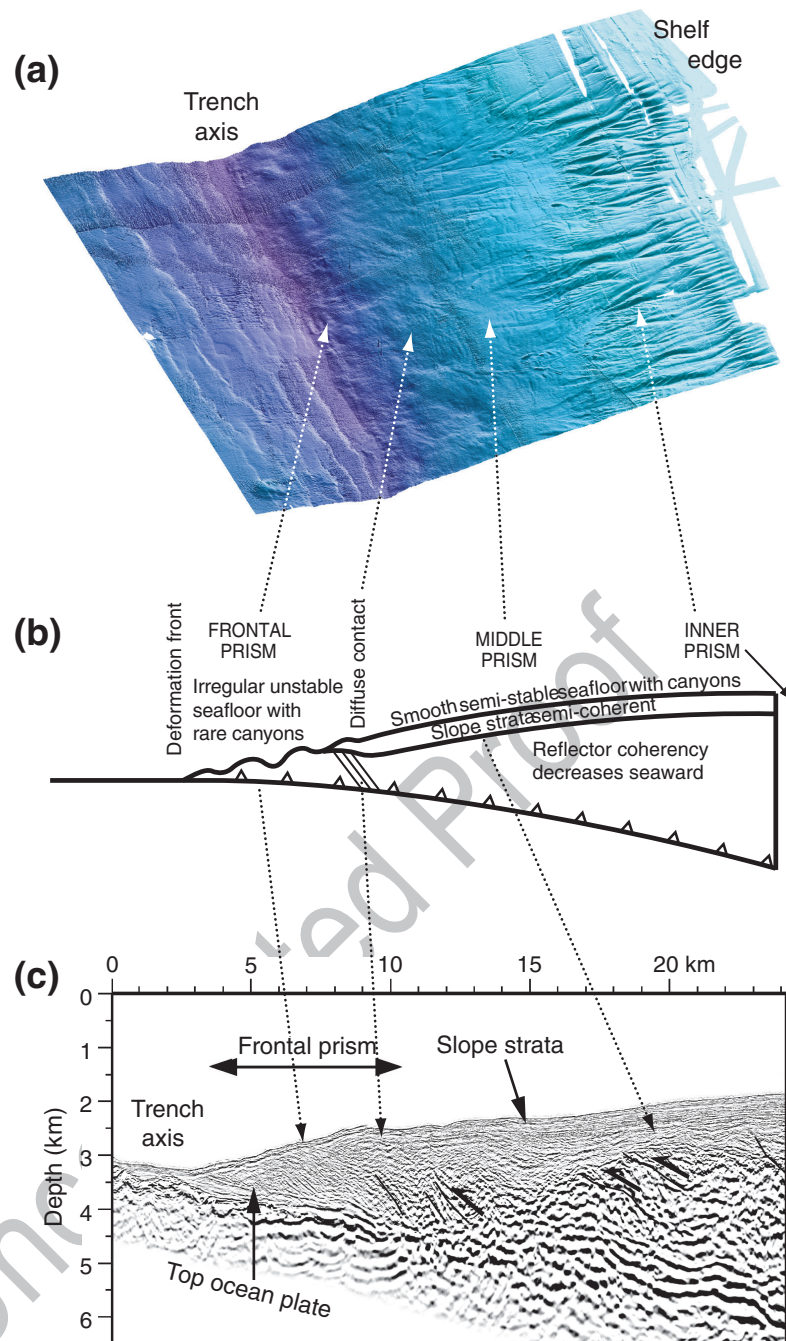
Although the clearest change from frontal prism to middle slope has been seen in erosional margins it is also observed in improved seismic images and high resolution bathymetry of accreting margins. Across the Alaska accretionary margin the contact between the frontal and middle prisms is defined by a change in structural vergence from landward to seaward (von Huene and Klaeschen, 1999). Strain and fluid venting were quantified across this margin along a transect just north of the Kodiak group of islands. The rate of permanent deformation peaks in the frontal prism and drops four-fold to the middle prism along with expulsion of all but 20% of original pore fluid (von Huene

and Klaeschen, 1999). Therefore middle prism strain must be largely elastic because it is associated with increased friction and microearthquake activity. The division between aseismic and seismogenic segments of convergent margin plate interfaces is consistent with segmentation. As mentioned previously, improved data across the “classical Sunda accretionary prism” (Hamilton, 1988) is separated into two prisms that back against a margin framework (Kopp and Kukowski, 2003). Wide-angle and reflection seismic images along with multibeam bathymetry show a little deformed slope apron covering a middle prism core containing Eocene rock. A splay fault system separates the middle slope from seafloor ridges of the frontal prism composed of material with low seismic velocity. This splay fault system produces a low continuous ridge along the 600 km lateral extent of the multibeam bathymetry acquired. Recent multibeam bathymetry and 3D seismic images across the Nankai margin show a splay fault system separating the active accreting frontal prism and a middle prism (Bangs et al., 2006; Moore, 2007). Forearc basin sediment on the middle prism is cut by numerous normal faults. The middle prism taper is shallower than the frontal prisms. Similar tectonic structure is observed along the accretionary Makran margin (Fruehn et al., 1997; Kopp et al., 2000; Kukowski et al., 2001), the Cascadia off central Oregon (Gedom et al., 2000), and south-central Chile (Ranero et al., 2006). A transition from the middle prism to the margin framework is observed in the canyon morphology that commonly diminishes sharply from the framework to the middle prism seafloor. Along the Chilean margin this corresponds to a change from landward dipping to seaward dipping faults (Ranero et al., 2006). Despite many second-order variations, a basic margin segmentation can be recognized in many recently acquired seismic images and multibeam bathymetry.

#### 3.1 Width of Frontal Prisms

Most seismic images of frontal prisms show compressional structure and imbrication. Single seismic lines can be very misleading because damage to frontal prism structure from high relief plowing into the subduction zone can add more complexity than is resolved even with modern seismic acquisition. A multibeam

**Fig. 2** The frontal prism, the middle (transition) prism, and the continental framework. (a) perspective view of multibeam bathymetry off northern Costa Rica from the trench to the shelf edge. The rough frontal prism seafloor without gullies is separated from a smoother middle prism with gullies and many small normal fault scarps. This morphology transitions to an upper slope with older and more sharply incised canyons. (b) Diagram of major features in the 2-prism model. (c) Pre-stack depth migrated seismic reflection image showing subsurface structure at a vertical exaggeration of 1.5 $\times$ . Note abrupt change in prism taper. (After Ranero et al., 2007.)



morphology map view is helpful in understanding such complexity and how damaged zones heal. Frontal prisms are restored only to their original width and appear to be self limiting. Global observations indicate a restricted range in frontal prism width. Their taper

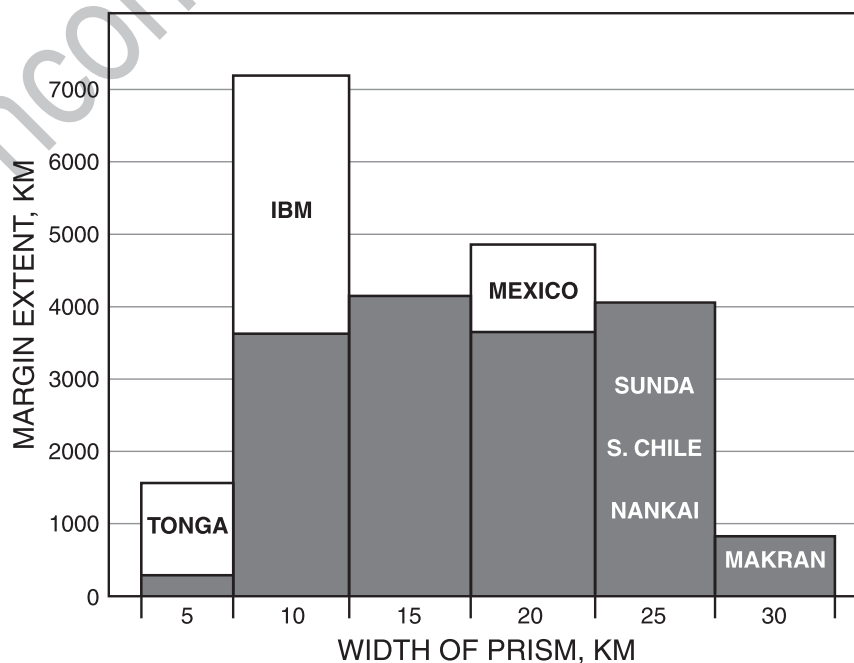
and volumes measured in undistorted seismic depth images are not readily available so we approximated frontal prism size using prism width (Table 1, Fig. 3). A prism's landward contact was located using several of the following criteria.

**Table 1** Compilation of geologic information on convergent margins used in Fig. 5

Global compilation of frontal prism width						
Margin sector	Length, (km)	Sed. Input (km)	Frontal prism	Middle prism	Subduct. Sed	Numb. lines multibeam
S. Chile	1,110	2.9	27	19		2 & mb
Chile 3-J to JFR	1,665	2	18	12	1.3	7 & mb
Chile JFR to Anto	1,445	0.4	10		1	6 mig + 5, mb
Peru N of Nazca	1,220	0.7	15		0.9	7 & mb
Middle America	1350	0.6	9		1	9 & mb
Mexico	1350	0.9	18		0.4	3 & mb
S Oregon	200	2	7	24	1.5	1 & mb
Oregon	770	4	14	9	2	2 & mb
NE Alaska	450	2	23	30	1.3	2 & mb
Kodiak-Shumigan	900	2	24	8	0.8	2 & mb
Aleutian to 180°	1,300	2	20	10		4
Kuril	1,320	0.7	14		0.8	4
N Japan	720	0.6	15		0.9	6 & mb
Nankai	700	1.3	24	52	1.1	6 & mb
Makran	900	7	30	250–350	3	1 & mb
Sunda Arc	2,500	1.5	22	75		4 & mb
<i>IBM</i>	3,500	0.5	10			2
<i>Tonga</i>	1,350	0.4	7			1 & mb

Column 2 – length km – is the extent of each margin. Column 3 – sed input km – is the trench sediment thickness at the deformation front. Column 4 – frontal prism – is the width of the frontal prism. Column 5 gives the width of the middle prism where present. Column 6 – subduct. sed – is the subducted sediment layer thickness in km where clearly defined. Column 7 – numb. line multibeam – is the number of transects available to establish thicknesses and extent of features – mb indicates where multibeam bathymetric information is available. The sum does not include IBM (Izu-Bonin-Mariana) which are italicized to indicate that information is not sufficient to meet standards used for margins listed above.

**Fig. 3** Global compilation of frontal prism widths. Bars are widths from images that clearly constrain the frontal prism. The compilation includes seismic images across about 48% of margins globally excepting areas of collision and where convergence is more oblique than 30°. Unshaded areas show data with less certain widths because of inadequate seismic image quality



A change from relatively smooth to rough seafloor morphology commonly at a scarp.

A sharp change from little deformed to deformed and obscure slope apron strata.

A transition from semi-coherent to non-coherent basement reflectors of eroding margins.

Change of taper, physical properties, or an increased horizontal velocity gradient

An abrupt break in age or rock type indicating a tectonic boundary

Prism widths along convergent margins (Fig. 3) were estimated from more than 70 selected seismic records and from multibeam bathymetry. Their trench axis parallel extent was estimated from satellite derived bathymetry. Subducting ridges and areas with more than 30° oblique convergence were avoided. The compilation of clearly bounded prisms includes 48% of convergent margins globally. Insufficient information is available to assess the Tonga and Izu-Bonin-Mariana frontal prisms with the certainty desired. Nonetheless, because of their great lateral extent, the average of their sparse available data is shown (Fig. 3) to indicate how including them might affect the compiled data. The frontal prisms of margins currently eroding are on average about ~15 km wide whereas the currently accreting margins are about ~22 km wide. As noted by Cliff and Vannucchi (2004) accreting margins commonly occur where convergence is less than 60 km/Myr and erosion occurs where convergence is more rapid. The Chile margin south of Valparaiso is an exception. Accretion south of Juan Fernandez Ridge became rapid as trench sediment fill thickness jumped from 1 km to more than 1.5 km (Onken et al., 2006). Accretion is a Pleistocene-Quaternary mode of tectonism following a Miocene period of dominantly erosional tectonism. Despite 70 km/Myr convergence, thick Pleistocene sediment is associated with current accretion showing that trench sediment thickness can overwhelm subduction channel capacity even where convergence is rapid.

Frontal prisms adapt readily to changes in the subducting seafloor morphology. Large embayments in the deformation front form as high relief on the lower plate subducts. These embayments return to their previous margin configuration as relief passes and are rapidly filled. Along the Costa Rican margin, the frontal prism embayments from subducting seamounts roughly 20 km in diameter and perhaps 2 km high heal in less than 0.2 Ma (von Huene et al., 2000). After

accelerated erosion over the Nazca Ridge off Peru, the margin re-establishes its frontal prism in ~4 Myr (von Huene et al., 1996). The filling of embayments stops when pre-collisional conditions are re-established.

The restricted width of frontal prisms globally indicates that they are at an optimum size for the current convergence rate, mode of sedimentation, and taper. The self limiting indicators in nature were observed in sandbox modeling where different modes of material transfer became constant after adjusting to the given conditions (Kukowski and Onken, 2006).

Frontal prisms at erosional and sparsely sedimented margins probably contain abundant slope sediment as contrast to trench sediment building a dominantly accretionary prism. Thus the greater median width of accreted margin frontal prisms may reflect the influence of differing prism materials and manner of accumulation. If the frontal prism accretes sediment, its increased width is adjusted by shifting the frontal and middle prism contact seaward. In narrowing margins the frontal prism contact shifts landward. From our analysis we derive three principal observations: (1) Frontal prisms occur at both erosional and accretionary margins; (2) Frontal prism width is commonly between 5 to 30 km and rarely wider. (3) Frontal prisms appear to be self-limiting in accord with prevailing structure, material, and dynamics.

#### 4 Observed Relation of Trench Sediment Thickness and Tectonic Processes

We now explore convergent margin kinematics, in particular the different environments associated with processes of accretion and erosion. Both accretion and erosion result from plate convergence so what differences in mass flux are associated with either tectonic type? Along the Chile subduction zone the effects of trench sediment supply and rate of plate convergence are well displayed. This subduction zone includes extremes from a sediment starved trench along its northern desert (<0.5 km thick trench sediment) to a sediment flooded (>1.5–3 km) trench settings along its glaciated southern coastal mountains. The effects of over- and under-abundance of sediment can be compared on either side of two ocean ridges that obstruct sediment transport down the northward deepening

trench axis. Across the Juan Fernandez Ridge the change in trench sediment thickness of adjacent segments is 2 km. Across the South Chile Rise triple junction a four-times reduction in plate convergence allows a longer time for trench sediment deposition. South of the triple junction trench sediment 3.5 km thick has been imaged whereas just north the sediment is about 1 km thick. These areas were surveyed with extensive multibeam bathymetry and depth processed reflection and wide angle seismic data as summarized in Ranero et al. (2006). The empty trench off northern Chile illustrates a type example of an erosional margin.

### 4.1 The North Chile Example of a Erosional Margin

The northern Chile geophysical data includes precise aftershock locations of the 1995 Antofagasta earthquake ( $M_w = 8.0$ ) recorded with a land-sea seismometer network (Fig. 4) (Husen et al., 2000; von Huene and Ranero, 2003; Sallares and Ranero, 2005). Multibeam bathymetry images canyons beginning on the shelf that deepen across the upper slope and are displaced by landward dipping normal faults (Fig. 3).

Down slope this morphology merges into a middle slope smoothed by mass wasting debris cut by seaward dipping normal faults. The lower slope is characterized by broad ridges that are continuous with sharp well developed lower plate horsts extending into the subduction zone (Fig. 4).

The seaward dipping normal faults of the middle prism extend 4 km into basement where they merge along a detachment. Analysis of the detachment fault geometry with methods applied to slide bodies (Watts and Grilli, 2002) shows low frictional strength (von Huene and Ranero, 2003). Fractures permeate the entire upper plate basement. Mass-wasting debris migrates down slope and accumulates in a well developed frontal prism. The prism's 3.5 km/s P wave velocity indicates >15% fluid (Sallares and Ranero, 2005) and the geometry of conjugate faults (Davis and von Huene, 1987) indicates a strength similar to frontal prisms of accretionary margins composed of water rich trench sediment. The upper plate's crystalline inner prism has seismic velocities of 5 km/s along the coast and continental shelf, ~4.5 km/s in the mid-slope, and 3.5 km/s velocities beneath the lower slope without an apparent change in rock type.

Along northern Chile and other erosional margins, the contact between framework rock and the frontal prism is commonly a transition from coherent basement

AU2

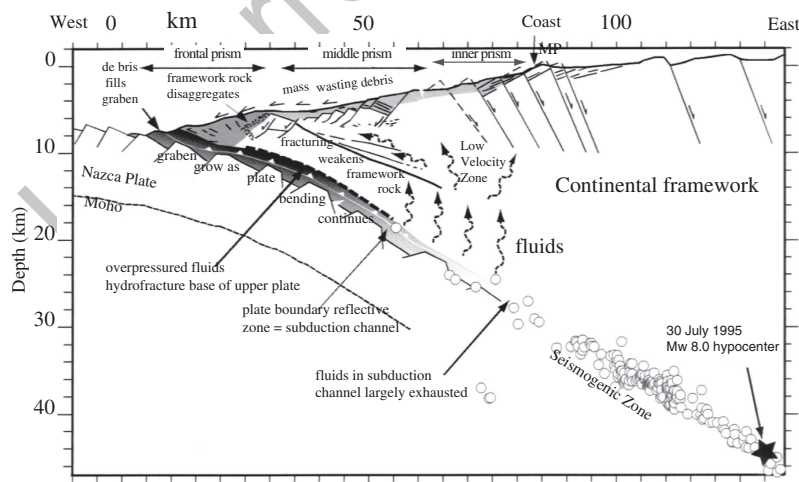


**Fig. 4** Diagram of subduction erosion along the north Chile margin. In the upper plate, a decreasing rock strength is associated with 3 tectonic styles across the slope. Landward-dipping normal faults develop perhaps as material loss down slope progressively removes a constraining mass. In the middle slope seaward dipping normal faults develop from gravity tectonics in weakened framework rock. Mass wasting debris collects in

a frontal prism and elevates pore fluid pressure allowing subduction of unconsolidated clastic debris. Clastic debris and basement fragments are inferred to fill a subduction channel. Normal faulting continues in the subducted ocean crust to accommodate continued plate bending in the subduction zone. (After von Huene and Ranero, 2003, Sallares and Ranero, 2005.)

reflections across the middle prism to a structureless seismic image (cf. Ranero and von Huene, 2000). The continuity of reflections weakens and fades away across the transition from a middle slope to the lower slope morphology. The middle slope morphology of fault scarps, rills, and ridges ends at the frontal prism where underlying slope reflectors decompose or break into short segments. Multibeam bathymetry commonly resolves frontal prism limits with better resolution than seismic images (cf. von Huene and Ranero, 2003).

Observations along the north Chile margin (von Huene and Ranero, 2003; Sallares and Ranero, 2005) reveal that: (1) erosional margins have frontal prisms that presumably elevate pore fluid pressure immediately above the underthrust lower plate and facilitate subduction of the slope materials spilling into the trench axis. (2) the upper plate framework rock decreasing P velocity seaward indicates material weakness to values found in middle prisms of accretionary margins; and (3) up-dip of the seismogenic zone, where slip is dominantly stable, the interplate fault is weakly coupled like those of accretionary margins. Slope material dominates the frontal prism and the subduction channel.

The crystalline basement ends at a transitional contact with a frontal prism, a contact that has been termed

a “backstop.” That term was formulated from concepts of accretionary wedges where the backstop is stationary (Byrne et al., 1988; Byrne et al., 1993). Along eroding margins this gradational contact migrates landward as material is removed. Despite its elegant simplicity and popular usage, the stable backstop concept does not apply here since over the long term erosional margins are extensionally faulted and material is removed rather than pushed or backed up against a rigid “bulldozer blade.”

## 4.2 Trench Turbidite Thickness and Tectonics at the Juan Fernandez Ridge

The aseismic Juan Fernández Ridge (JFR), a seamount chain on the Nazca plate, subducts beneath the Central Chilean continental margin. The continental sediment source and plate convergence are the same on either side of the subducting ridge and only trench sediment volume changes. The crest of the subducting JFR uplifts the entire continental slope (Fig. 5) (Ranero et al., 2006; Laursen et al., 2002; von Huene et al., 1997). In the

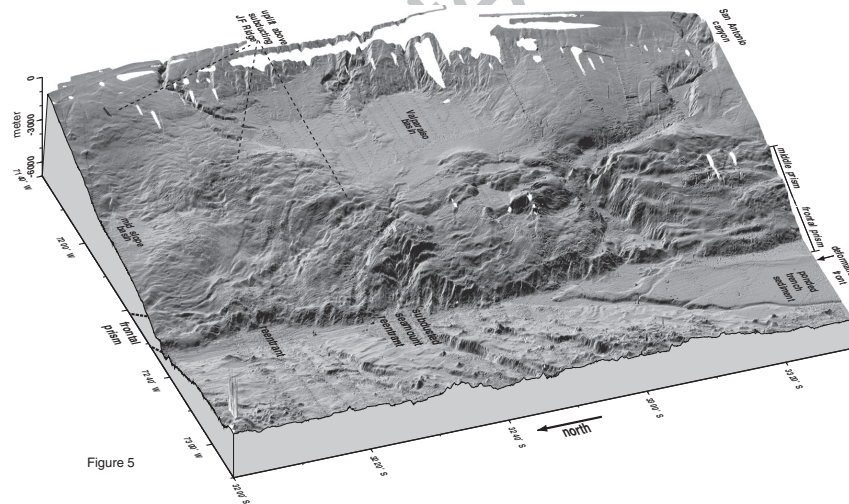


**Fig. 5** Multibeam bathymetry of the central Chile margin where Juan Fernandez Ridge subducts. The ridge crest blocks axial sediment transport thereby separating a thickly sedimented from a modestly sedimented trench axis. After the ridge subducts its subducted continuation is marked by a low ridge diagonally crossing the slope. Frontal prism ridge and trough morphology

south of Juan Fernandez ridge is replaced by a disorganized morphology north. The middle slope breaks-up over the trailing flank of the southward migrating ridge. Some sediment input to the subduction zone to the south accretes but north all sediment subducts despite the same rate of plate convergence. (After Ranero et al., 2006.)

trench the ridge relief impedes axial transport of sediment resulting in rapid sediment deposition upstream (south) and only modest sediment accumulation on the downstream (north) side. This results in accretion of trench sediment upstream, and essentially complete sediment subduction downstream (Ranero et al., 2006). The subducting ridge separates an erosional slope morphology to the north from an accretionary one to the south. The eroding continental slope frontal prism is 5–10 km wide and is presumed to reduce interplate friction so that all trench sediment subducts. Fluids from the subducted sediment escapes at the back of the frontal prism forming 100-m-high mud diapirs (Ranero et al., 2006). Once it has formed the frontal prism does not widen significantly as shown by more than 200 km of multibeam bathymetry north of the subducting ridge. A middle slope erosional margin morphology extends 1000 km north through the area off Antofagasta and beyond (von Huene and Ranero, 2003).

South of the JFR the trench axis contains >2 km of sediment, and a 10–25 km wide frontal prism. The ~20 km wide middle prism is covered by a little deformed seafloor. Sediment accretion is the dominant process along the lower slope and a 1.0–1.5 km thick layer of the lower trench sediment section subducts beneath the frontal prism (von Huene et al., 1997; Diaz-Naveas, 1999). Variants of this pattern extend southward for ~1500 km to where tectonics are modified by the subduction of the South Chile Rise (Bangs and Cande, 1997; Diaz-Naveas, 1999).

The thickness of sediment at the deformation front correlates with accretion and erosion. The upper sediment accretes and the bottom 1 km subducts as also noted by other investigators (Le Pichon et al., 1993; Clift and Vannucchi, 2004; Kukowski and Onken, 2006).

### 4.3 Effect of Convergence Rates Observed Across the South Chile Rise

Accretion and erosion on either side of the South Chile Rise illustrates the effects of convergence rate on tectonics (Fig. 6). South of the triple junction where the spreading South Chile Rise subducts, the Antarctic plate converges with South American at ~18 mm/year whereas north of the Rise convergence is 84 mm/year or roughly five times more rapid. The northward migrating Chile Rise collision left a truncated continental

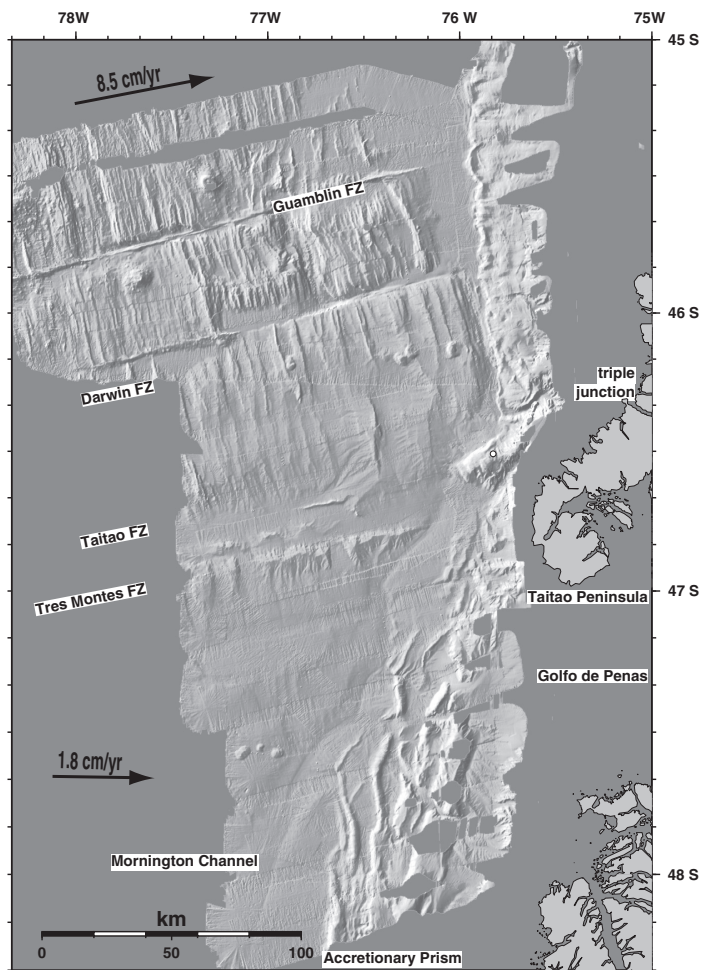
margin in the south. After the Chile Rise relief subducted, the continental slope subsided and sediment in the trench thickened and widened (Ranero et al., 2006). About 100 km south of the triple junction where the South Chile Rise subducted ~3–6 Myr ago, the frontal and middle prisms are ~60 km wide (Fig. 6). Slow convergence rates reduce sediment subduction and trench sediment has more time to accumulate. Where the Chile Rise currently collides with the continental margin, the frontal prism is only ~5 km wide (Bourgeois et al., 2000; Behrmann et al., 1994). North of the Chile Rise where convergence is rapid, the trench deepens and has a relatively thin sediment fill (~1.5 km). The frontal prism here is ~10–15 km wide and sediment subduction is efficient (Bangs and Cande, 1997) (Fig. 6). Thick and thin trench sediment are associated with wide and narrow frontal prisms. The shallow dip of the subducting crust may also influence prism width. But a first order association is trench sediment thickness and prism width which here is a function of convergence rate.

## 5 Subduction Channel Character

The subduction channel, a layer directly below the plate interface, was originally conceived as filled with a slurry of sheared material (Shreve and Cloos, 1986). However, drilling through the frontal prism encountered narrow fault zone above little deformed sediment (cf. Kimura et al., 1997), consistent with recent seismic images (cf. Kinoshita et al., 2006). This called for modification of the original fluid mechanics analogy. At the Ecuadorian margin, good continuity and strong reflections allows exceptional velocity determinations from which physical properties estimates are derived (Calahorrano et al., 2008). Indicated is a division of the channel into 3 zones similar to upper plate segments. Such a segmentation is also proposed by Vannucchi et al. (2008) from study of a fossil subduction channel on land. The 3 zones of Calahorrano et al. (2008) indicate conditions in currently active subduction channel and the “Shallow, Intermediate and Deep” segments of Vannucchi et al. (2008) show a corresponding structure at outcrop scale. The channel character varies if sediment smoothes the subducting seafloor topography or if rough irregular seafloor has subducted (Sage et al., 2006).

AU3

**Fig. 6** Multibeam bathymetry at the triple junction of the south Chile Rise collision zone. Circles are ODP Leg 141 drill sites (Behrmann et al., 1994) and *numbered lines* are RC2902 seismic images (Ranero et al., 2006). The finger of land in the middle-right is the Taitao Peninsula opposite which the Chile Rise subducts. South of the Chile Rise convergence is slow allowing more time for trench sediment deposition. The resulting thick sediment enhances accretion as shown by the growth of ridges as the triple junction migrates north. Northward, where the margin is dominantly erosional, the trench axis is bordered by a narrow frontal prism backed against the margin framework. (From Ranero et al., 2006.)



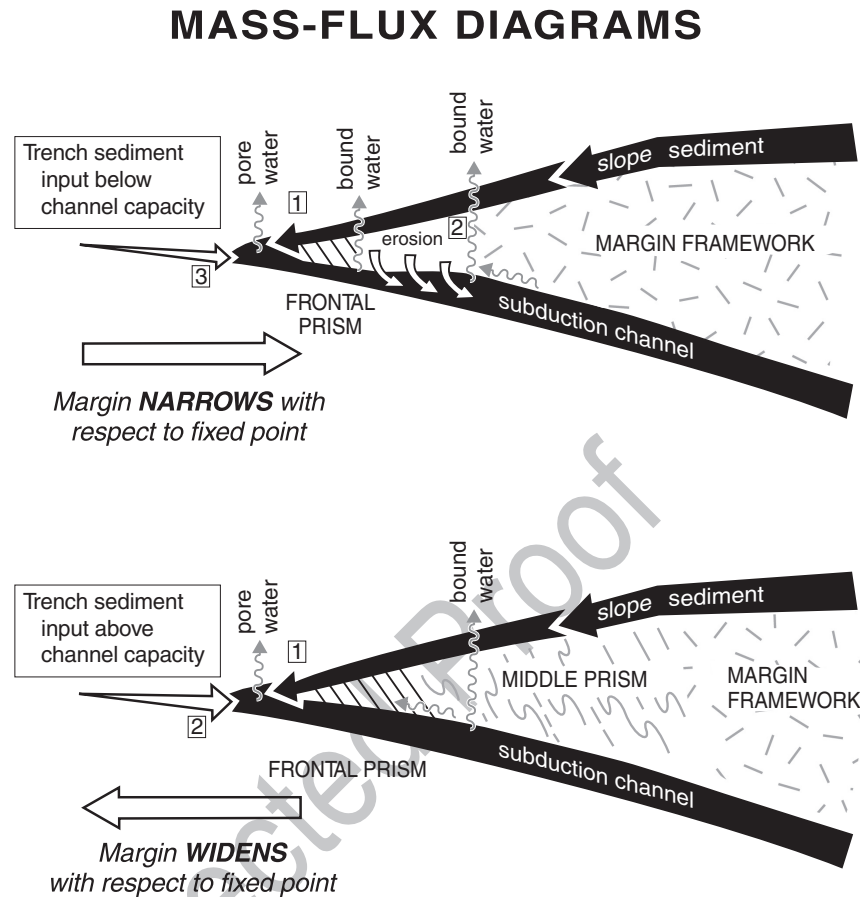
In many seismic images, a minimally deformed stratified trench fill subducts beneath the frontal prism decollement. The decollement is locally a sharp reflection (cf. Bangs et al., 2006; Moore, 2007). Drill cores and logs off Costa Rica show a narrow interplate fault zone (20–30 m) at the top of a little deformed and under-consolidated sediment section (Kimura et al., 1997; Saffer, 2003). Compared with drainage paths from the frontal prism, fluid of the subduction channel must drain through a longer path and therefore dewatering is inferred to be slower.

Zone I of Calahorrano et al. (2008) and the shallow segment of Vannucchi et al. (2008) occur beneath the frontal prism. Seismic velocities increase rapidly in a landward direction from 1.8 to 2.6 km/s indicating relatively rapid fluid drainage but slower than from the overlying frontal prism. A weak interplate fault running through weak materials is consistent with little

recorded microseismicity along the decollement. In rock outcrops, deformation is mainly extensional and the many small fractures probably served as conduits for fluid drainage. Quartz and calcite veins are absent. Vannucchi et al. (2008) propose accommodation of strain by pervasive failure along many small fractures during compaction.

Beneath the middle prism the channel image is commonly 3 or 4 thick (150–500 m) high-amplitude-low frequency reflections. The loss of resolution results from an increased sonic footprint with depth (Fresnell zone), increased attenuation and scatter of reflected high frequency energy. The change from the first to second zone or segment is transitional or abrupt. Off Ecuador the seismic velocity within this segment of the subduction channel stays relatively constant at 2.8 km/s and it is commonly a low velocity zone (Sage et al. 2006; Calahorrano et al., 2008). Sometimes

**Fig. 7** Subduction channel mass transport. **TOP** Trench sediment thickness is less than subduction channel thickness and the contact between framework rock and the frontal prism migrates landward with respect to a fixed point. Material is input to the subduction channel from (1) the slope, (2) from basal erosion, and (3) at the deformation front. **BOTTOM** Trench sediment thickness exceeds subduction channel thickness and the excess accretes. Material input to the subduction channel is mainly at the deformation front. As the margin widens frontal prism material transfers to the middle prism and the prism contact migrates seaward



refraction data modeling yields thinner low velocity zones than the high amplitude-low frequency reflection images appear to indicate (Christeson et al., 1999; Takahashi et al., 2000). Perhaps the fault zone at the top of the channel is associated with concentrated fluids. In the absence of lower plate relief the reflective zone thickness is uniform indicating little internal slip. Differential subduction rates along thrust faulted segments within the channel would result in variable channel thicknesses. Seismic velocities in the second zone (Calahorrano et al., 2008) indicate a 28% porosity, more grain-to-grain contact, an increased rigidity, and a reduced rate of fluid drainage. Fluids that vent at the middle slope seafloor have the chemistry of chemically bound water released by clay dehydration reactions in underthrust sediment (Hensen et al., 2004). Inferred coseismic high fluid pressure pulses along the plate interface (Ranero et al., 2008) are interpreted to cause the hydrofracturing that facilitates basal erosion beneath the subsiding middle slope.

Beneath middle prisms the upper boundary images are commonly clear but not the lower boundary. Local sharp lower boundaries may indicate a floor thrust in addition to the roof thrust (cf. Sage et al., 2006; Lohrmann et al., 2006). A floor thrust was observed in outcrops of the subduction channel (Vannucchi et al. 2008).

Outcrops of the intermediate segment show a dense arrays of extensional calcite veins. The fault displacement occurs by many repeated small events and vein structure indicates cyclic fluid pressures (Vannucchi et al., 2008). The floor thrust begins to lock locally and produce contractile structure.

Zone II transitions into zone III where high amplitude plate interface reflectivity weakens and disappears (Ranero et al., 2008). It is also a region in which teleseismically recorded earthquakes nucleate. The loss of reflectivity and impedance contrasts is interpreted as decreased porosity and greater interplate friction. Calahorrano et al. (2008) point out that overburden loads are great enough to cause elastic deformation of

clastic grains (70 to 110 MPa). The change from aseismic to seismogenic behavior appears to correspond with reduced fluid, increased compaction, and increased rigidity.

In outcrop, the extensional structure is overprinted by contractile deformation (Vannucchi et al., 2008). Temperature indicators approach 150°C which is the temperature inferred to mark the seismogenic zone. Locking of the floor thrust becomes evident and the roof thrust locks intermittently. Cyclic behavior is observed in the structure of veins and is inferred to show changes within earthquake cycles. Similar faults have been observed in rock outcrops of the Kodiak Island group of Alaska (Rowe, 2007).

Where abundant seafloor relief or ridges subduct, the thickness and physical properties of the subduction channel vary spatially. Over highs covered with little subducting sediment the porosity decreases more rapidly than across adjacent lows with thicker than normal sediment (Sage et al. 2006). Summit areas of subducting highs show erosion whereas surrounding lows have thick sediment. A probable differential friction in response to topography produces the implied patchiness off Ecuador (Sage et al., 2006) and the isolated centers of seismic activity of southeastern Costa Rica (Protti et al., 1995; Bilek and Lay, 2002; Bilek et al., 2003).

The original subduction channel concept analogues to fluid mechanics of a slurry now appears to include a multifaceted mechanical system. The zone of high amplitude reflections represents coherent stratification imaged with current techniques beneath the frontal prism and locally into the middle prism. This indicates a coherent mass at a stratal resolution of about a hundred meters. A small body of modern and fossil data show the expected increase in rigidity and friction with depth along the plate interface fault and reflectivity indicates that fluids drain until channel material has the seismic velocity of hard rock. This occurs roughly where aseismic behavior changes to seismogenic behavior (Ranero et al., 2008).

## 6 Updating the Subduction Channel Concept

The two prisms and a subduction channel of the original model are consistent with current observations. Since the concept was introduced, multiple inputs to

the channel in addition to trench sediment, the structure of the major tectonic components, a lower material strength, and low interplate fault friction in the aseismic segment have been observed. Multiple inputs to the subduction channel up-dip of the seismogenic zone are: (1) the slope materials captured at the frontal prism seafloor and cycled through it, (2) chemically bound water released from subducting materials as temperatures and pressure increase, and (3) the clastic debris from basal and frontal erosion.

Observations of interplate and internal friction were measured along landslide slip planes that extend to the plate interface (von Huene et al., 2004) and derived from conjugate faults (Davis and von Huene, 1987). Critical taper, when constrained properly, indicates that interplate friction beneath the frontal prism is less than the static internal friction measured in samples (Wang and Hu, 2006; von Huene and Ranero, 2003; Lallemand et al., 1994). Strength of the material in a margin derived from taper have often been averaged beyond the area at critical taper. Disorganized and unstable seafloor of the frontal prism indicates an area at critical taper whereas the more stable middle slope commonly does not meet the critical taper criterion of a slope at or near failure. Interplate friction beneath the frontal prism derived from taper and fault geometry are as much as an order of magnitude less than assumed in the original model. Interplate friction sufficiently low for all trench sediment to subduct is observed in seismic images and was drilled at the Costa Rican margin (Kimura et al., 1997). Subduction of unconsolidated trench sediment beneath a poorly consolidated frontal prism requires the low basal friction consistent with “aseismicity” along the decollement of the frontal prism.

Channel thickness is a major uncertainty in quantifying the mass-flux of the subduction system. The low velocity plate interface reflective sequences associated with the subduction channel are considered indicators of hydration (Park et al., 2002). Hydration could extend above the channel into the fractured upper plate or below the channel into a porous upper ocean crust making a determination of thickness ambiguous. If interplate faults impede fluid migration at the top of the subduction channel, a zone of more concentrated fluid would occupy the thinner zone interpreted in wide angle seismic data (Christeson et al., 1999; Takahashi et al., 2000).

An indication of channel thickness is also derived from the mass required to balance material removed by

basal subduction erosion to cause slope subsidence. A rate of material removal estimated from subsidence and convergence rates yields a subduction channel thickness (cf. Vannucchi et al., 2003, 2004; Scholl and von Huene, 2008). A nominal channel thickness estimate is roughly the 1 km lateral average of the high amplitude reflective layer.

## 7 Discussion

A unifying “framework” concept of convergent margin tectonics can be developed around the thickness of trench sediment, segmentation, a modified subduction channel concept, low interplate friction of the aseismic zone, and dynamic changes during an earthquake cycle.

### 7.1 Tectonics and Trench Sediment Abundance

Trench sediment abundance commonly correlates with accreting or eroding tectonics. In the subduction channel model a balance between channel capacity and the abundance of trench sediment is a first order control. Where trench sediment volume and plate convergence rate have been steady for million year periods, all trench sediment less than ~1 km thick subducts whereas a 2-km-thick trench sediment nearby loses the upper 0.5–1 km by accretion. This approximation appears to hold globally (Clift and Vannucchi, 2004). Short periods of disrupted axial sediment transport leave a less obvious record.

The mechanisms that control subduction zone channel thickness in nature are not fully understood. In studies of convergent margin tectonics with sandbox experiments, varying the height of a gate at the back of the box varies the subduction channel layer thickness (Lallemand et al., 1994; Kukowski and Onken, 2006; Lohrmann et al., 2006). When the gate opening equals the thickness of the sand layer representing trench sediment, all sand at the deformation front subducts whereas a greater or lesser gate opening allows erosion or accretion. Such a relationship between trench sediment and subduction channel thickness is seen in nature but an analogous controlling feature is not yet

obvious. Mass flux control points along the subduction zone that have been identified in seismic images are few and imaging in this region requires the most powerful available techniques and a relatively simple geology. Some associations indicate possible controls. The middle prism where relatively rapid rates of subsidence are observed is probably a channel capacity control area. Another may result from character of the subducting plate. The subduction channel varies in thickness locally from basement relief and subducted horsts the height of the channel are overlain by a thin channel. Material strength above and below the plate interface fault zone and lithostatic load are probable controls. However until active subduction channels are sampled and physical properties are measured, understanding will probably advance with laboratory experiments and numerical modeling. Notwithstanding uncertainties regarding controlling mechanisms, the balance between subduction channel thickness and trench axis sediment thickness is a first order control of erosion and accretion.

### 7.2 Upper Plate Strain and Interplate Friction

During earthquakes the dynamic friction of the seismogenic zone is presumably less than its friction during interseismic periods. Friction on faults during an earthquake are difficult to quantify and synthetic modeling or wave-form analysis commonly do not include fluid pressure pulses, opening and closing of fractures, and frictional heating including local flash-melting. The low fault and material strength in the frontal prism revealed by conjugate faults probably shows its dynamic strength during earthquakes. It is plausible that unstable morphology of the frontal prism forms principally during coseismic deformation. During interseismic periods deformation might occur from aseismic fault displacement and gravity tectonics. In the dynamic wedge theory, critical state is achieved during coseismic deformation in frontal prisms (Wang and Hu, 2006).

The paradox of a converging plate compressional environment and yet many small normal faults across the middle prism is most easily explained by transitory relaxation of the elastic strain during of shortly after an earthquake. When periodically relaxed sufficient for

small extensional displacements to occur, normal faults will grow incrementally. The oscillation of compression and brief extension can occur during earthquake cycles.

### 7.3 The Limited Width of the Frontal Prism

A mechanism that limits frontal prism width is indicated by our compilation (Fig. 3). Self limiting is clearly observed where subducting seamounts form embayments. These breached areas fill very rapidly but only to their previous width. The narrow frontal prism above the 2 Km high subducting Nazca Ridge returns to its previous width in ~4Myr. Rapid accretion that stops at a limit requires a change in controlling processes. A possible explanation involves the progressive change in physical properties up slope. In the trench axis, sediment has a normal vertical seismic velocity gradient that increases with depth. It parallels a vertical gradient of strength from weak at the top to relatively stronger at the bottom. This velocity/strength relation was measured in drill cores at DSDP site 499 in the Middle America Trench axis where the shear strength increased from near zero just below the seafloor to ~50kPa at 200m. In the same interval the seismic velocity increased ~300m/s (Shipboard Party, 1982). At the deformation front of accreting margins the deep material that subducts is stronger than the shallower material that detaches and forms the overlying frontal prism. Even where all sediment subducts, the velocity gradient across the decollement steps from a lower one above it to a higher one below it (Saffer, 2003). After a clear decollement forms, the subducted section still retains its stratified structure and relatively greater strength whereas the weaker sediment of the frontal prism above it deforms. During some period of the earthquake cycle the decollement must be the weakest element in the system and yet one that at times is stronger than the prism in order to drive imbricate faulting.

Detailed velocity information from pre-stack depth migration processing (i.e., von Huene et al., 1998) shows that pore fluid in the frontal prism drains rapidly as the frontal prism thickens tectonically. On the other hand, below the plate interface the subducted sediment must drain through a longer path that retards fluid drainage and presumably development of greater sediment strength. As a margin wedge develops, the upper

plate strength may increase faster than the subduction channel's and as this continues the step to a higher velocity across the decollement could disappear. Where the subduction channel is a clear low velocity the step has inverted. The interplate fault beneath the middle prism probably collects water released by clay dehydration from the subduction channel as described earlier. The relative plate velocity shift occurs at or near the contact between the frontal and middle prisms.

If velocity is a proxy for material strength then the middle prism may be as strong or stronger than the subduction channel when averaged over multiple earthquake cycles. If the subduction channel and the interplate fault become relatively weak, the shear strength from subduction becomes insufficient to produce much permanent compressional deformation in the upper plate. Fully understanding the interplay between upper and lower plate strength and that of the interplate shear during an earthquake cycle will require better resolution in spatial and temporal observations. Relative strength and dynamics in the frontal and middle prism transition is an interesting candidate explanation.

### 7.4 Dynamics

An interplay between state of stress and strength of the interplate fault zone are explained in the Dynamic Coulomb wedge theory (Wang and Hu, 2006). The Dynamic Coulomb wedge contains a frontal and middle prism with dissimilar bulk rheology. Therefore stress during a seismic cycle affects each segment differently. During interseismic periods the middle slope segment and the continental framework store elastic strain (Fig. 8b). Low relative rates of permanent deformation occur in the middle prism and framework because they can store more elastic strain than frontal prisms. During an earthquake the released elastic strain extends the mid slope segment and it shoves against the frontal prism creating a transient coseismic pulse of rapid deformation and elevated pore fluid pressure (Fig. 8a).

In many studies a time averaged steady state deformation is assumed. However, the variation in stress between interseismic and coseismic periods is significant as seen in the stress drop during an earthquake. Peak stress is the most likely time that major permanent

AU4

deformation occurs. Physical parameters such as those from fluid migration will vary locally during an earthquake as waves of fluid pressure migrate along a rupture plane and change its strength profile. In fact it has been suggested that the plate interface becomes an aquatard during interseismic periods and with the release of strain it becomes an aquifer during and shortly after an event. Multibeam bathymetry with resolution greater than seismic reflection images shows structure from the most recent tectonics which best link it to current seismicity.

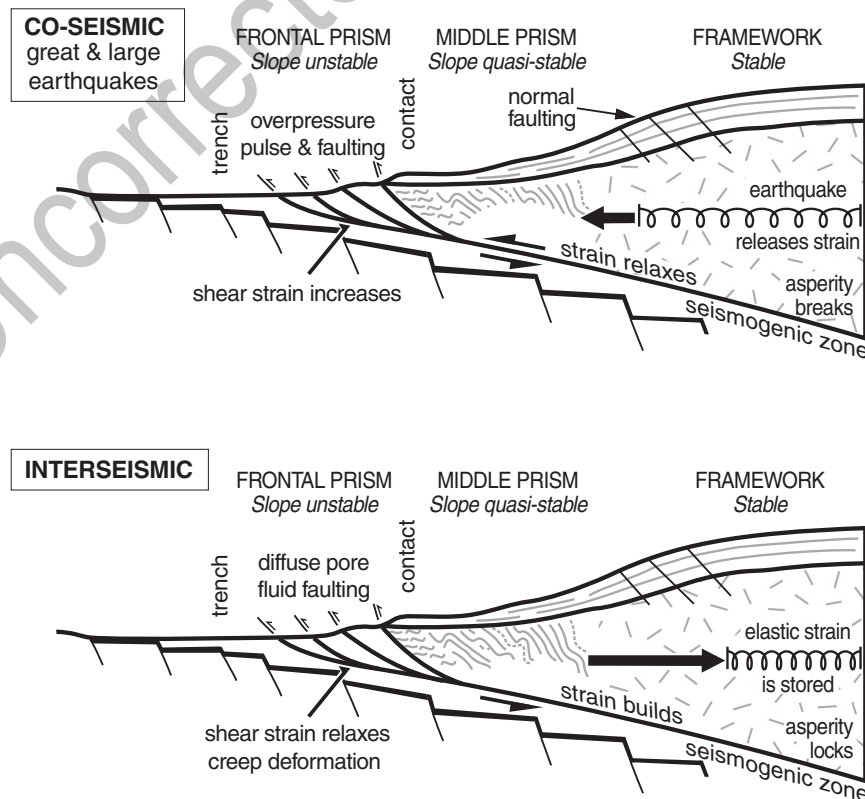
The mechanics of eroding and accreting margins are probably more similar than commonly envisioned (i.e., Stern, 2002) considering the following. (1) Both accreting and eroding margins have frontal prisms of similar width. (2) The taper angles  $\alpha$  versus  $\beta$  (Lallemand et al., 1994) if restricted to depth processed seismic records, scatter  $4^\circ$  or  $5^\circ$  along single margins whereas the maximum difference between accretionary and erosional margins is only  $8^\circ$  (von Huene and Ranero, 2003; Wang and Hu, 2006). Thus taper variability in a single margin can be half of the extreme difference between

accretionary and erosional end-member tapers. (3) Frontal prism strength of each type is similar. Strength derived from angular relations of conjugate faults for the erosional northern Chile frontal prism lies between the values for the accretionary Aleutian and Oregon prisms and is the same as that of Nankai. (4) Locations of modeled  $100\text{--}150^\circ\text{C}$  isotherms are locally similar with respect to seismicity (Oleskevich et al., 1999).

Different seafloor morphologies apparent in multi-beam bathymetric perspective diagrams probably reflect dominance of one middle prism tectonic process for longer periods or subduction of major seafloor relief as at Juan Fernandez Ridge. Although the rocks comprising each margin are petrologically different, a more dominant factor in end-member tectonics is the degree of framework rock fracturing in eroding margins and sediment consolidation in accreting ones. Locally, accretion and erosion interchange readily.

Material difference in a frontal prism appear to influence tectonics minimally. The few estimates from analysis of conjugate faults and landslide geometry show that a frontal prism of mass wasting rubble and a

**Fig. 8** Diagram illustrating the dynamic Coulomb Wedge theory (Wang and Hu, 2006). Elastic strain builds in the wedge beneath the middle and upper slope during the interseismic period (*lower*) and is released during the coseismic period (*upper*). Earthquake rupture propagating into the aseismic area will shove against the frontal prism and cause a pulse of deformation resulting in the seafloor instability revealed in high resolution multibeam bathymetry



prism of trench sediment have similar dynamic strengths (von Huene and Ranero, 2003; Wang and Hu, 2006).

## 8 Summary

Improved geophysical imaging has revealed structure that was obscure during early development of convergent margin models. With new information we draw ideas about accretion and erosion closer together in a more unified framework concept. The conventional “accretionary wedge” is resolved into three structural segments. A rapidly deforming frontal prism is separated by a splay fault or transitional contact from a moderately stable middle prism that in turn grades into a relatively stable inner prism of coherent margin framework structure. Eroding margins are also resolved into three segments beginning with a frontal prism structured like that of accreting margins and a similar inner prism. The moderately stable middle prism is commonly cut by normal faults, it has a reduced seismic velocity, and its morphology clearly differs from the parent margin framework of the inner prism. This tripartite framework characterizes most seismic images acquired with large modern systems and processed in depth, especially when integrated with multibeam bathymetry. Segmentation corresponds with an aseismic frontal region where few if any plate interface earthquakes are recorded that becomes seismogenic beneath the middle prism or inner prism.

The upper plate’s basal boundary is the plate interface fault separating it from the underlying subduction channel. The channel is a layer of trench sediment and erosional debris on top of oceanic basement. The subduction channel is segmented as shown in a recent studies of seismic data and in studies of a fossil subduction channel in outcrops on land. These results indicate a division that roughly matches segments of the upper plate. The subducted material begins as a stratified sequence and its seismic velocity down dip is consistent with a progressive consolidation as would be expected. Much of the channel clastic material is stratified and not a slurry as originally conceived. A multifaceted mechanics can be anticipated once more detailed structural evidence and physical properties are resolved.

The mass flux (material movement and its source) and inferred mechanics are specific to each segment.

Frontal prisms add relatively small volumes of material to a margin especially when composed of mostly repositioned slope materials. They widen or narrow readily in response to changes in character of the subducting plate: in other words they can accrete or erode in response to a rough or smooth subducting seafloor. Their widths are commonly within a 5–30 km range globally and their constrained width, whether a trench axis is sediment flooded or starved, indicates a self limiting mechanism. Processes in the frontal prism reduce friction sufficient to allow subduction of soft trench sediment beneath poorly consolidated prism sediment. A fault within weak materials is weak, consistent with absence of plate interface seismicity.

Eroding and accreting middle prism are differentiated based on structure and mass flux. At accreting margins the frontal prism’s highly deformed sediment is tectonically added to the middle prism which may in turn become part of the upper plate’s older margin framework. At eroding margins, framework rock structure is commonly imaged down slope to the actively deforming frontal prism. However, seismic velocity much lower than its framework rock parent indicates pervasive fracturing across eroding margin middle prisms. Thus the greatest difference between eroding and accreting margins are observed in middle prisms whereas the frontal prism and inner prism seismic images are similar.

The subduction channel concept offers a simple and practical framework to visualize convergent margin mass flux. When trench axis sediment is thicker than subduction zones can accommodate the surplus material accretes, and when thinner the margin erodes. Observations indicated that trench sediment greater than  $\sim 1 \pm 0.5$  km thick is associated with accretion and less than  $\sim 1 \pm 0.5$  km thick with erosion, thereby generally bracketing channel thickness. This is consistent with thickness of high amplitude reflective sequence along plate boundary that is presumed to be the subduction channel (e.g., Nankai, Bangs et al., 2006; Ecuador, Sage et al., 2006). The relation between trench sediment thickness and subduction channel thickness is a first-order control on whether the margin’s dominant mass flux is erosional or accretionary.

Eroding and accreting margins may be composed of different materials but their frontal prism width and critical tapers, plate interface friction, subduction channel thickness, porosity, and modeled temperature

profiles are similar at current scales of investigation. Stress drops during earthquake rupture are similar so the plate interface dynamic strength and fluid pressures could reach similar peak values in both margin types. Physical properties derived from structure appear similar and it is peak dynamic forces that are most likely to shape major tectonic features.

The kinematic subduction channel concept is consistent with the Dynamic Coulomb Wedge theory (Wang and Hu, 2006) which specifies the time frame within which processes occur. The two prism time varying dynamic model can remove the paradox of an eroding margin with an “accretionary structured” imbricated frontal prism. It provides a better understanding of how plate convergence can be coeval with active normal faulting of the middle slope given the oscillatory relaxation of contractile strain during seismic cycles. Erosional and accretionary margins have more similar features than often inferred and it is the middle prism that displays basic rock and mechanical differences.

The tectonic effects of different inter-plate mass transfer schemes with regard to seismicity and tsunamis have been argued without an emerging consensus. Lack of consensus emphasizes the need for finer resolution in controlled source seismic data and a need for scientific drilling into plate interfaces to significantly advance understanding of convergent margin dynamics.

**Acknowledgements** We appreciate the discussions with Kelin Wang that greatly improved earlier manuscripts. R. Ranero is supported by Repsol. R von Huene received a USGS Bradley fellowship to help support this work.

## References

- Bangs, N.L., and S. Cande, (1997), The episodic development of a convergent margin inferred from structures and processes along the southern Chile margin. *Tectonics*, 16 (3), 489–505
- Bangs, N.L.B., S.P.S. Gulick, and T.H. Shipley, (2006), Seamount subduction erosion in the Nankai Trough and its potential impact on the seismogenic zone. *Geology*, 34 (8), 701–704, doi: 10.1130/G22451.1
- Behrmann, J.H., S.D. Lewis, S.C. Cande, and ODP Leg 141 Scientific Party, (1994), A synthesis of results from Leg 141 of the Ocean Drilling Program. *Geol. Rundsch.* 83, 832–852
- Bilek, S.L., S.Y. Schwartz, and H.R. DeShon, (2003), Control of seafloor roughness on earthquake rupture behavior: *Geology*, 31 (5), 455–458
- Bilek, S.L., and T. Lay, (2002), Tsunami earthquakes possibly widespread manifestations of frictional conditional stability. *Geophys. Res. Lett.* 29. p. art. No. 1673 Behrmann, J.H., S.D. Lewis, S.C. Cande, and ODP Leg 141 Scientific Party, (1994), A synthesis of results from Leg 141 of the Ocean Drilling Program. *Geol. Rundsch.* 83, 832–852
- Bond, C.E., A.D. Gibbs, Z.K. Shipton, and S. Jones, (2007), What do you think this is? “Conceptual uncertainty” in geoscience interpretation. *GSA Today* 17, doi 10.1130/GSAT01711A
- Bourgeois, J., C. Guivel, Y. Lagabriele, T. Calmus, J. Boulegue, and V. Daux, (2000), Glacial-interglacial trench supply variation, spreading-ridge subduction, and feedback controls on the Andean margin development at the Chile triple junction area (45–48°), *J. Geophys. Res.* 105, 8355–8386
- Byrne, D.E., D.M. Davis, and L.R. Sykes, (1988), local and maximum size of thrust earthquakes and the mechanics of the shallow region of subduction zones, *Tectonics* 7, 833–857
- Byrne, D.E., W.H. Wang, and D.M. Davis, (1993), Mechanical role of backstops in growth of forearcs, *Tectonics*, 12, 123–144
- Calahorrano, B., V. Sallares, J.-Y. Collot, F. Sage, and C. Ranero, (2008), Nonlinear variations of the physical properties along the southern Ecuador subduction channel: Results from depth-migrated seismic data; *Earth and Planet. Sci. Lett.* 267; 453 doi:10.1016/j.epsl.2007.11.061
- Christeson, G.L., K.D. McIntosh, T.H. Shipley, E.R. Flueh, and H. Goodde, (1999), Structure of the Costa Rica convergent margin, offshore Nicoya Peninsula, *J. Geophys. Res.*, 104, 25, 443–25 468
- Christeson, G.L., N.L. Bangs, and T.H. Shipley, (2003), Deep structure of an island arc backstop, Lesser Antilles subduction zone, *J. Geophys. Res.* 108 (B7), 2327, doi:10.1029/2002JB002243
- Clift, P.D., and P. Vannucchi, (2004), Controls on tectonic accretion versus erosion in subduction zones: Implications for the Origin and recycling of the continental crust. *Rev. Geophys.*
- Cloos, M., and R.L. Shreve, (1988), Subduction channel model of prism accretion, melange formation, sediment subduction, and subduction erosion at convergent plate margins: 2. Implications and discussion, *Pageoph*, 129, (3/4), 501–545
- Davis, D.M., and R. von Huene, (1987), Inferences on sediment strength and fault friction from structures of the Aleutian Trench, *Geology* 15, 517–522
- Diaz-Naveas, J.L., (1999), Sediment subduction and accretion at the Chilean convergent margin between 35° and 40° S, PhD dissertation, Christian-Albrechts-Universität zu Kiel, 130 p.
- Fruehn, J., R.S. White, and T.A. Minshull, (1997), Internal deformation and compaction of the Makran accretionary wedge, *Terra Nova* 9, 101–104
- Gerdom, M., A.M. Trehu, E.R. Flueh, and D. Klaeschen, (2000), The continental margin off Oregon from seismic investigations, *Tectonophysics* 329, 79–97
- Hamilton, W., (1988), Plate tectonics and island arcs, *Geol. Soc. Am. Bull.* 100, 1503–1527
- Hensen, C., K. Wallmann, M. Schmidt, C.R. Ranero, and E. Suess, (2004), Fluid expulsion related to mud extrusion off Costa Rica –a window to the subducting slab, *Geology* 32, 201–204

AU5

- Husen, S., E. Kissling, and E.R. Flueh, (2000), Local earthquake tomography of shallow subduction in north Chile: A combined onshore and offshore study, *J. Geophys. Res.* 105, 28, 183–28,198
- Kimura, G., E. Silver, et al., (1997), *Proceedings Ocean Drilling Program Initial Reports, Volume 170*, 458 p. (U.S. Government Printing Office, Washington, D.C.)
- Kimura, G., Y. Kitamura, Y. Hashimoto, A. Yamaguchi, T. Shibata, K. Ujiie, and S. Okamoto, (2007), Transition of accretionary wedge structures around the up-dip limit of the seismogenic subduction zone, *Earth Planet. Sci. Lett.* 255, 471–484, doi:10.1016/j.epsl.2007.01.005
- Kinoshita, M., G. Moore, R. von Huene, H. Tobin, and C.R. Ranero, (2006), The seismogenic zone experiment, in Burger and Fujioka, eds, *The impact of the Ocean Drilling Program, Oceanography*, vol. 19, No. 4, p
- Kopp, H., and N. Kukowski, (2003), Backstop geometry and accretionary mechanics of the Sunda margin, *Tectonics*, 22 (6), 1072, doi:10.1029/2002TC001420
- Kopp, H., J. Fruehn, E.R. Flueh, C. Reichert, N. Kukowski, J. Bialas, and D. Klaeschen, (2000), Structure of the Makran subduction zone from wide-angle and reflection seismic data, *Tectonophysics*, 329, 171–191
- Kukowski, N., T. Schillhorn, K. Huhn, U. von Rad, S. Husen, and E. Flueh, (2001), Morphotectonics and mechanics of the central Makran accretionary wedge off Pakistan, *Marine Geology*, 173, 1–19
- Kukowski, N., and O. Onken, (2006), Subduction Erosion – the “Normal” Mode of Fore-Arc Material Transfer along the Chilean Margin?; *The Andes*, Springer, Berlin, Heidelberg New York; pp. 216–236
- Lallemant, S.E., P. Schnurle, and J. Malavieille, (1994), Coulomb theory applied to accretionary and nonaccretionary wedges: Possible causes for tectonic erosion and/or frontal accretion: *J. Geophys. Res.*, 99 (B6), 12, 033–12,055
- Laursen, J., D.W. Scholl, and R. von Huene, (2002), Neotectonic deformation of the central Chile margin. Deepwater forearc basin formation in response to hot spot ridge and seamount subduction, *Tectonics*, 21 (5), 1038 doi:10.1029/2001TC901023
- Le Pichon, X., P. Henry, and S. Lallemant, (1993), Accretion and erosion in subduction zones: The role of fluids, *Annu. Rev. Earth Planet. Sci.* 21, 307–331
- Lohrmann, J., N. Kukowski, C. Krawczyk, O. Onken, C. Sick, M. Sobiesiak, and A. Rietbrock, (2006), Subduction Channel Evolution in Brittle fore-Arc Wedges – a Combined Study with Scaled Sandbox Experiments, Seismological and Reflection Seismic Data and Geological Field Evidence: *The Andes*, Springer, Berlin, Heidelberg New York; pp. 237–262
- Moore, G.F., (2007), Three-dimensional Splay Fault Geometry and Implications for Tsunami Generation, *Science* 318, 1128, DOI: 10.1126/Science.1147195
- Oleskevich, D.A., R.D. Hyndman, and K. Wang, (1999), The updip and down-dip limits to great subduction earthquakes: Thermal and structural models of Cascadia, South Alaska, SW Japan, and Chile, *J. Geophys. Res.* 104 (14), 965–14, 997
- Oncken, O., D. Hindle, J. Kley, K. Elger, P. Victor, and K. Schemmann, (2006) *Deformation of the Central Andean Upper Plate System – Facts, Fiction, and Constraints for Plateau Models; The Andes*, Springer, Berlin, Heidelberg New York; pp. 3–27
- Park, J.-O., T. Tsuru, N. Takahashi, T. Hori, S. Kodaira, A. Nakanishi, S. Miura, and Y. Kaneda, (2002), A deep strong reflector in the Nankai accretionary wedge from multichannel seismic data: Implications for underplating and interseismic shear stress release, *J. Geophys. Res.* 107 (B4), 10.1029/2001JB000262
- Protti, M., F. Guendel, and K. McNally, (1995), Correlation between the age of the subducting Cocos plate and the geometry of the Wadati-Benioff zone under Nicaragua and Costa Rica, in Mann, P. ed., *Geologic and Tectonic Development of the Caribbean Plate Boundary in Southern Central America: Geol. Soc. Am. Special Paper 295*
- Ranero, C.R., and R. von Huene, (2000), Subduction erosion along the Middle America convergent margin, *Nature* 404, 748–752
- Ranero, C.R., R. von Huene, W. Weinrebe, and C. Reichert, (2006), Tectonic processes along the Chile convergent margin, in: *The Andes, active subduction orogeny*, Onken, O. and 7 others, eds, Springer verlag, Berlin-Heidelberg-New York, pp. 91–122
- Ranero, C.R., R. von Huene, W. Weinrebe and U. Barckhausen, (2007), *Convergent Margin Tectonics of Middle America: A Marine Perspective*, in *Central America: Geology, Resources and Hazards*, (2007), Jochen Bundschuh and Guillermo E. Alvarado, eds, Taylor and Francis, London, Volume 1, pp. 239–265
- Ranero, C.R., I. Grevemeyer, H. Sahlíng, U. Barckhausen, C. Hensen, K. Wallmann, W. Weinrebe, P. Vannucchi, R. von Huene, and K. McIntosh, (2008), The hydrogeological system of erosional convergent margins and its influence on tectonics and interplate Seismogenesis, *Geochem. Geophys. Geosyst.* 9 (1), 1–18, Q03S04, doi:10.1029/2007GC001679
- Rowe, C., (2007), Comparison between Three Out-of-Sequence Thrusts from Japan and Alaska: Implications for Nankai Drilling Target from the Rock Record. *Scientific Drilling, special Issue No. 1*, pp. 82–83
- Saffer, D.M., (2003), Pore pressure development and progressive dewatering in underthrust sediments at the Costa Rican subduction margin: Comparison with northern Barbados and Nankai, *J. Geophys. Res.*, 1089B50,2261, doi:10.1029/2002JB001787
- Sage, F., J.-Y. Collot, and C.R. Ranero, (2006), Interplate patchiness and subduction-erosion mechanisms: Evidence from depth-migrated seismic images at the central Ecuador convergent margin, *Geology*, 34 (12), 997–1000; doi. 10.1130/G22790A.1
- Sallares, V., and C.R. Ranero, (2005), Structure and tectonics of the erosional convergent margin off Antofagasta, north Chile (23°30'S), *J. Geophys. Res.* 110 (B06101), doi:10.1029/2004JB003418
- Scholl, D.W., and R. von Huene, (2008), Crustal recycling at modern subduction zones applied to the past – issues of growth and preservation of continental basement, mantle geochemistry, and supercontinent reconstruction, in *Geol. Soc. Am. Memoir 200, 4-D Framework of Continental Crust* (edited by Robert D. Hatcher, Jr., Marvin P. Carlson, John H. McBride, and José Ramón Martínez Catalán)
- Shipboard Party, (1982), in Aubouin, J., and von Huene R., *Init. Repts DSDP, 67*, Washington DC (US Govt. Printing Office)
- Shreve, R.L., and M. Cloos, (1986), Dynamics of sediment subduction, melange formation, and prism accretion, *J. Geophys. Res.* 91, 10,229–10, 245

AU6

- Sorokhtin, O.G., and L.I. Lobkovskiy, (1976), The mechanism of subduction of oceanic sediments into a zone of underthrusting of lithospheric plates, *Izv. Acad. Sci. USSR Phys. Solid Earth, Eng. Transl.* 12, 289–293
- Stern, R.J., (2002), Subduction zones, *Rev. Geophys.* 40.4, 3–1–3–48, doi:10.1029/2001RG000108.
- Taira, A., (1994), When Plates Collide, *Convergent Margin Geology, Oceanus*, Winter 1993/94, p 95–98
- Takahashi, N., S. Kodaira, T. Tsuru, J.-O. Park, Y. Kaneda, H. Kinoshita, S. Abe, M. Nishino, and R. Hino, (2000), Detailed plate boundary structure off northeast Japan coast, *Geophys. Res. Lett.* 27 (13), 1977–1980
- Vannucchi, P., C.R. Ranero, S. Galeotti, S.M. Straub, D.W. Scholl, and D. McDougall Ried, (2003), Fast rates of subduction erosion along the Costa Rica Pacific margin: Implications for non-steady state rates of crustal recycling at subduction zones, *J. Geophys. Res.* 108: doi 10.1029/2002JB002207
- Vannucchi, P., S. Galeotti, P.D. Clift, V.R. Ranero, and R. von Huene, (2004), Long term subduction erosion along the Middle America Trench offshore Guatemala, *Geology* 32, 617–620
- von Huene, R., and D. Klaeschen, (1999), Opposing gradients of permanent strain in the aseismic zone and elastic strain across the seismogenic zone of the Kodiak shelf and slope, Alaska, *Tectonics*, 18, 248–262, doi:10.1029/1998TC900022
- von Huene, R. and C.R. Ranero, (2003), Subduction erosion and basal friction along the sediment-starved convergent margin off Antofagasta, Chile, *J. Geophys. Res.* 108 (B2), 2079, doi:10.1029/2001JB001569, 2003
- von Huene, R., I.A. Pecher, and M.A. Gutscher, (1996), Development of the accretionary prism along Peru and material flux after subduction of Nazca Ridge, *Tectonics* 15, 19–33
- von Huene, R., J. Corvalan, E.R. Flueh, K. Hinz, J.A. Korstgard, C.R. Ranero, W. Weinrebe, and the CONDOR Scientists, (1997), Tectonic control of the subducting Juan Fernandez Ridge on the Andean margin near Valparaiso, Chile, *Tectonics* 16, 474–488
- von Huene, R., C.R. Ranero, W. Weinrebe, and K. Hinz, (2000), Quaternary convergent margin tectonics of Costa Rica, segmentation of the Cocos Plate, and central American volcanism, *Tectonics* 19, m. 2, e14–334
- von Huene, R., C.R. Ranero, and P. Watts, (2004) Tsunamigenic slope failure along the Middle America Trench in two tectonic settings, *Mar. Geol.* 203, 303–317
- Watts, P., and S.R. Grilli, (2004), Tsunami generation by submarine mass failure I: Wavemaker modes, *J. Wtrwy, Port, Coast, and Oc. Engrg.*, ASCE
- Wang, K., and Y. Hu, (2006), Accretionary prisms in subduction earthquake cycles: The theory of dynamic Coulomb wedge, *J. Geophys. Res.* 111, B6, B06410, 16p, IOI 10.1029/2005JB004094

AU7

AU8

**Author Queries:**

AU1: Please check the name of the corresponding author for correctness.

AU2: This reference is not provided in the reference list. Please provide.

AU3: Reference has not been provided in the list. Please supply.

AU4: Reference has not been provided in the list. Please supply.

AU5: Please provide complete bibliographic details of this reference.

AU6: Please provide publisher name and publisher location.

AU7: We have inserted the authors name from net information. Please check.

AU8: This reference is not cited in text. Please provide.